

uncertainty still exists. A sensitivity study was made at numerous energies between 0.6 and 10.0 MeV in which all combinations of the phase shifts (given in columns 5, 6, and 7) $\pm 1^\circ$ were used to calculate the polarization distribution. The same was done for $\delta \pm 2^\circ$ above 10.0 MeV. Below 10 MeV it was found that the changes in the polarization at the angle near the positive maximum varied from the central value P_{pos} by about $\pm 0.03P_{\text{pos}}$. The study with the larger increment showed variations around $\pm 0.07P_{\text{pos}}$. If one considers the change in the average polarization for a 20° region centered near P_{pos} (a range typically used in polarization experiments) the effect is reduced by about 40%. Above 4 MeV there is also sizable (negative) polarization at forward angles. Since the cross section is relatively large here, this is the most efficient analyzing region. However, these sensitivity calculations show that the variations here are about

30% greater than those around P_{pos} . Thus, until more is known about the neutron-helium phase shifts, one is probably restricted to the region of the positive maximum for the more accurate investigations.

ACKNOWLEDGMENTS

The authors are indebted to M. M. Meier, R. S. Thomason, and Dr. L. A. Schaller for assistance in taking the data. We wish to thank Dr. F. O. Purser, Dr. W. Haeberli, Dr. G. R. Satchler, and Dr. R. B. Perkins for helpful discussions. Dr. N. R. Roberson and Dr. R. V. Poore are owed a debt of gratitude for their assistance with the on-line computer. Thanks are due to Dr. A. J. Elwyn for discussions and for allowing use of the potential-model calculations, which are in great part the product of his labor.

Proton-Proton Bremsstrahlung at 61.7 MeV*

M. L. HALBERT AND D. L. MASON†

Oak Ridge National Laboratory, Oak Ridge, Tennessee 37830

AND

L. C. NORTHCLIFFE‡

Texas A & M University, College Station, Texas 77843

(Received 6 November 1967)

The two final-state protons in the reaction $p+p \rightarrow p+p+\gamma$ at 61.7 ± 0.1 MeV were detected by $(\Delta E, E)$ telescopes placed at 30° on opposite sides of the beam. About 250 events were detected in a geometry with angular acceptance comparable to the maximum possible noncoplanarity. Additional data were obtained with apertures of smaller height, restricting the measurement to a more nearly coplanar geometry. The data indicate that the cross section is smaller for noncoplanar events. The estimated coplanar cross sections and differential cross section as a function of γ -ray angle are presented. The results agree with recent theoretical predictions.

I. INTRODUCTION

THE proton-proton bremsstrahlung (PPB) reaction, $p+p \rightarrow p+p+\gamma$, is of considerable current interest in the study of nuclear forces. The process involves different relative energies of the protons in the initial and final states and thus may provide information about matrix elements of the proton-proton interaction off the energy shell. Several years ago Sobel and Cromer¹ suggested that measurement of the PPB cross section might select among the different nucleon-nucleon potentials which describe elastic scattering equally well. The off-shell matrix elements enter

into nuclear-matter calculations, and, indeed, may be important for any system having more than two nucleons.

The process was first studied experimentally at 158 MeV by Gottschalk, Shlaer, and Wang.²⁻⁴ In their arrangement, often referred to as the Harvard geometry, the final-state protons were detected in coincidence by a pair of counter telescopes placed at equal angles on opposite sides of the beam. The total angle between the telescopes was less than that between scattered and recoil protons from p - p scattering so that elastic protons could not be detected in true coincidence. The energy of each proton was measured; with the known detector

* Research sponsored by the U. S. Atomic Energy Commission under contract with Union Carbide Corporation.

† Oak Ridge Graduate Fellow from the University of Florida under appointment from the Oak Ridge Associated Universities.

‡ Visiting scientist at Oak Ridge National Laboratory, 1965-66.

¹ M. I. Sobel and A. H. Cromer, Phys. Rev. **132**, 2698 (1963).

² B. Gottschalk, W. J. Shlaer, and K. H. Wang, Phys. Letters **16**, 294 (1965).

³ B. Gottschalk, W. J. Shlaer, and K. H. Wang, Nucl. Phys. **75**, 549 (1965).

⁴ B. Gottschalk, W. J. Shlaer, and K. H. Wang, Nucl. Phys. **A94**, 491 (1967).

angles and beam energy, this completely determined the kinematics of each PPB event. If E_L and E_R are the kinetic energies of the protons on the left and right sides of the beam, then for coplanar events with proton angles θ_L and θ_R the kinematically allowed values of E_L and E_R form a closed ring in a plot of E_L versus E_R . Noncoplanar events fall within this ring. Thus the position of a given event in the plane uniquely defines the γ -ray angles and energy so that detection of the γ rays is unnecessary. In the original measurements of Ref. 2, a γ -ray detector was used as additional confirmation that PPB events were being recorded. In subsequent experiments the γ -ray detector was omitted. Similar measurements have been reported at 48,^{5,6} 46,⁷ 33.5,⁷ and 30 MeV.⁸ In addition, measurements at 204 MeV with a different arrangement have been made by Rothe, Koehler, and Thorndike.^{9,10}

The work reported here was done at 61.7 MeV in the Harvard geometry, with both counter telescopes at 30° . This choice of beam energy was made with the intention of providing a new datum between 48 and 158 MeV. Since finite angular resolution smears out the kinematic ring, the polar-angle acceptance was made sufficiently small to ensure that coplanar events would form a well-defined ring. The role of noncoplanar events was also investigated.

The principal difficulty in these experiments arises from the rarity of PPB events in comparison with the enormous number of elastic protons incident on each counter. For the large-aperture geometry used in the present work, about 3×10^6 elastic protons entered each counter for every PPB event detected. Some of these elastic protons produce abnormally small pulses because of reactions in the detector, slit-edge penetration, etc. Accidental coincidences between these pulses may simulate PPB events. In previous work the beam current was kept small (< 5 nA) to minimize such accidentals. In this experiment most of the unwanted pulses were rejected by an energy-loss criterion, thereby permitting higher beam currents to be used.

II. EXPERIMENTAL METHOD

The proton beam from the Oak Ridge Isochronous Cyclotron (ORIC) was transported through the cyclotron vault by a quadrupole doublet, a uniform-field bending magnet, and a second doublet. Nondispersive deflection through 45° was achieved by requiring a horizontal focus halfway through the bending magnet.

⁵ R. E. Warner, Phys. Letters **18**, 289 (1965); **19**, 719 (1966).

⁶ R. E. Warner, Can. J. Phys. **44**, 1225 (1966).

⁷ I. Slaus, J. W. Verba, J. R. Richardson, R. F. Carlson, W. T. H. van Oers, and L. S. August, Phys. Rev. Letters **17**, 536 (1966).

⁸ J. C. Thompson, S. I. H. Naqvi, and R. E. Warner, Phys. Rev. **156**, 1156 (1967).

⁹ K. W. Rothe, P. F. M. Koehler, and E. H. Thorndike, Phys. Rev. Letters **16**, 1118 (1966).

¹⁰ K. W. Rothe, P. F. M. Koehler, and E. H. Thorndike, Phys. Rev. **157**, 1247 (1967).

The beam then passed through a 4-in.-diam hole in an 8-ft-thick concrete shielding wall into another room. A third quadrupole doublet brought the beam to a focus at the center of a 24-in.-diam scattering chamber, located 5 ft beyond the exit of the doublet. The only collimator was a pair of jaws before the second quadrupole to wipe off the top and bottom wings of the beam which would otherwise have struck the beam pipe close to the chamber. The mean energy of the cyclotron beam was shown to be 61.8 ± 0.1 MeV by directing the beam through a well-calibrated analyzing magnet. The energy spread of the beam was not determined. It was probably comparable with ± 0.1 MeV since repeated measurements with the 40-MeV beam from ORIC show a typical energy spread of $\pm 0.15\%$.¹¹

The width of the beam spot was first determined by moving a 0.003-in. nickel wire across the beam and measuring the elastic scattering yield at 90° as a function of wire position. This measurement showed that the full width at half-maximum was about 0.05 in., in agreement with calculations of the beam-transport system. The vertical height was estimated to be about 0.2 in. from these calculations. This was verified by viewing a phosphor placed at the center of the chamber and also by the darkening and activation of a glass plate exposed to the beam for a few minutes. The angular divergence was about $\pm 1.0^\circ$ horizontally and considerably less vertically, as estimated from exposures of glass plates several feet beyond the center of the chamber.

In later runs the beam spot on the phosphor appeared similar and the study with the wire was not repeated. It was found that $(90 \pm 5)\%$ of the beam was transmitted through a slit 0.065 in. wide and 0.20 in. high inserted at the center of the chamber. A split ion chamber was placed at the exit of the chamber as a continuous monitor of horizontal beam wandering. On the average the beam remained centered within 0.01 or 0.02 in.; larger fluctuations of short duration associated with cyclotron instability were occasionally noted. The beam was stopped in an evacuated Faraday cup 4 ft beyond the center of the chamber.

A general view of the apparatus is shown in Fig. 1. The scattering chamber was filled with hydrogen gas of high purity (< 10 ppm total impurities). The pressure was maintained slightly above atmospheric. A window of 0.0015-in. aluminum 4 in. from the chamber center separated the gas from the cyclotron vacuum. Fresh gas was flowed continuously through a liquid-nitrogen trap at a rate sufficient to change the contents of the chamber twice per hour. The energy loss of the beam in the Al window and the 4 in. of gas was very nearly 0.1 MeV; therefore the measurements pertain to an energy of 61.7 ± 0.1 MeV.

The target volume is the portion of the beam seen by a pair of $(\Delta E, E)$ counter telescopes geometrically

¹¹ M. L. Mallory and S. S. Stevens (private communication).

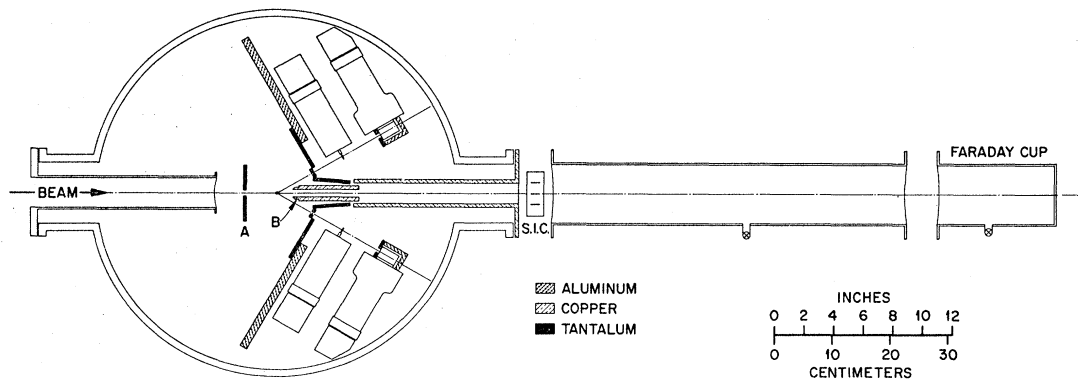


FIG. 1. Experimental arrangement viewed from above. The shield A prevents illumination of the telescope apertures by protons scattered in the entrance window. The baffles B stop protons scattered elastically from beyond the active volume. The split ion chamber is designated by S. I. C.

defined by slits and rectangular apertures made of $\frac{3}{16}$ -in. Ta, as shown in Fig. 2. The centers of the apertures lay in a plane containing the beam axis. The dimensions and telescope acceptance angles are given in Table I. The telescopes could be remotely positioned to within 0.1° , and were set at 30.0° for the data reported here.

For convenience in the following discussion, we adopt a spherical coordinate system, with its polar axis along the beam direction and its origin at the center of the scattering chamber. Because of the finite aperture height the average values of the polar angles θ_L and θ_R are slightly larger than 30.0° (about 30.3° for the large aperture geometry).

The limiting polar-angle acceptance of $\pm 2.7^\circ$ quoted in Table I may not give an accurate idea of the effective angular resolution. Consider a particular pair of angles (θ_L, θ_R) . The corresponding geometrical efficiency is proportional to the length of the target volume over which events with these angles can be detected. Median-plane events with $\theta_L = \theta_R$ are registered with full efficiency only between 29.3° and 30.7° . Beyond these angles the efficiency decreases to zero as the limits 27.3° and 32.7° are approached. For $\theta_L \neq \theta_R$, the efficiency is always smaller than for $\theta_L = \theta_R$, and the limits are even more restricted—for example, it is impossible to detect both protons from $(30^\circ, 28.2^\circ)$ or $(30^\circ, 31.8^\circ)$ events.

The azimuthal angles of the two protons φ_L and φ_R are measured relative to the median plane of the aperture¹²; a proton in this plane has $\varphi = 0^\circ$ if it enters the right telescope and $\varphi = 180^\circ$ in the left telescope. For any PPB event the angle of noncoplanarity, Φ , is given by

$$\Phi = \varphi_L - \varphi_R - 180^\circ. \quad (1)$$

A coplanar event is specified by $\Phi = 0$.

¹² The azimuthal angle φ is the angle between the median plane and the component of proton velocity normal to the beam axis. In Ref. 4, the symbol φ has a different meaning.

The detectors were rectangular plastic scintillators. Each was viewed edge-on by a photomultiplier, type 6342A for the ΔE counters and 8054 for the E counters. The ΔE scintillators were 0.055 in. thick, while the thickness of the E scintillators was 1.25 in., sufficient to stop 62-MeV protons. The width and height were 0.38 and 1.25 in. for the ΔE detectors, and 0.75 and 2.25 in. for the E detectors.

Signals from the ΔE counters triggered a coincidence circuit with a resolving time of 30 nsec, adequate to guarantee that prompt coincidences would be registered only by protons from the same beam burst, since the rf period was 44.5 nsec. Coincidences opened a pair of linear gates for a period of 40 nsec to pass the E signals to amplifiers for stretching and amplification. The amplifiers in turn were connected to a 20 000-channel two-parameter analyzer. Prompt coincidences were stored in the upper 100×100 portion of the analyzer memory. At the same time, random coincidences between protons from adjacent beam bursts were stored in the lower half of the memory. This was done by use of a duplicate coincidence circuit, with the ΔE_L signal delayed by one rf period. Compensating delays were inserted where necessary to maintain proper gate timing. As a check on the operation of the analyzer, the number of coincident E signals presented to the analyzer was determined by a separate coincidence circuit and compared with the total number of events stored in the memory. This comparison showed that the analyzer was storing all events.

As mentioned above, some elastic protons give abnormally small pulses in the E counters and accidental coincidences between these pulses can simulate PPB events. The protons scattered elastically at 30° (46 MeV) can be distinguished from the bremsstrahlung protons (15–25 MeV), since the latter lose more energy in the ΔE counters. By adjustment of the discriminator threshold for each ΔE pulse, about 99% of the elastic protons in each telescope were prevented from triggering the coincidence circuits without rejecting bremsstrah-

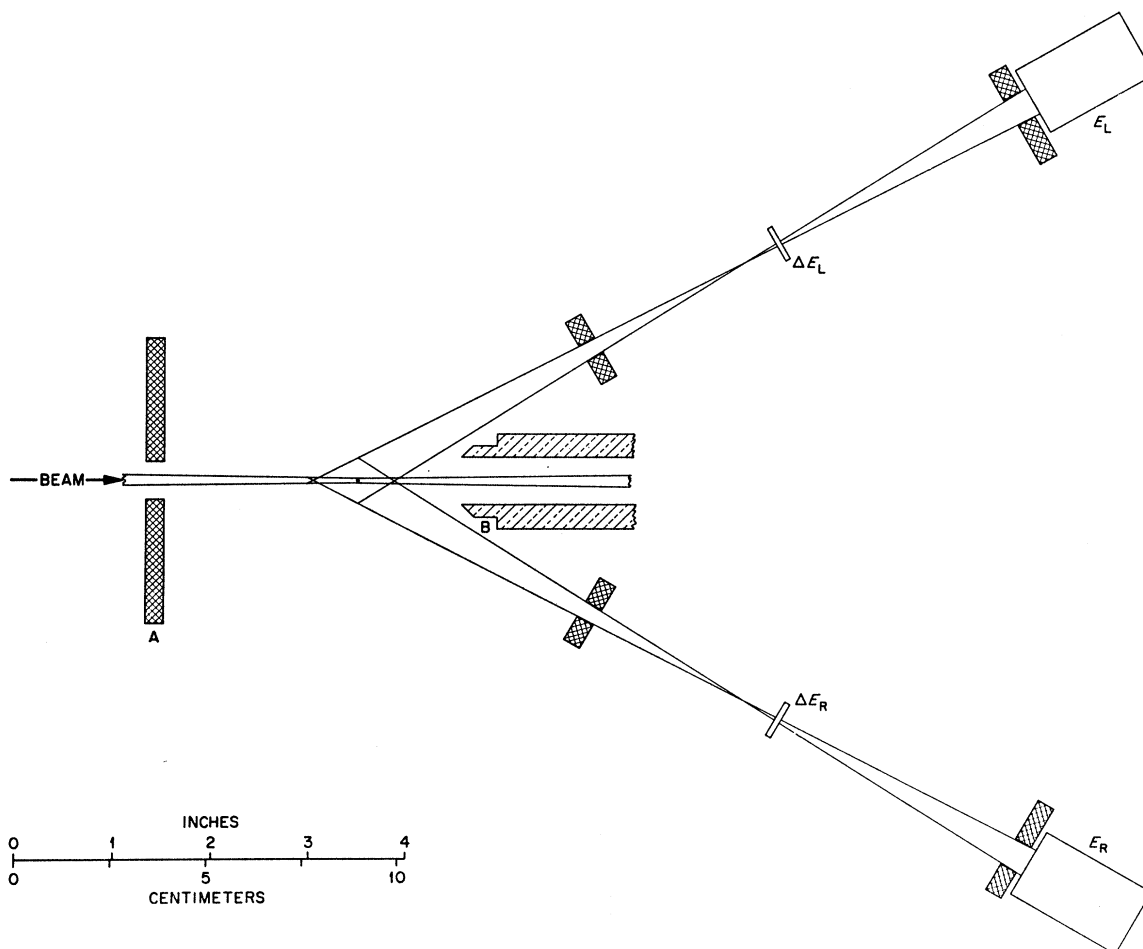


FIG. 2. Detailed view of detector and slit geometry as viewed from above. The outline of the beam envelope represents the boundary of the region of half-maximum intensity.

lung protons. The discrimination against the elastic protons would have been more nearly complete with a higher threshold, but it was felt that acceptance of a few elastics could be tolerated to be certain that no significant number of bremsstrahlung events were rejected. This method could not eliminate accidental coincidences between low-energy protons, such as might arise from stray beam striking the entrance apertures. These events were minimized by careful placement of the shield A (see Fig. 1) and the telescope collimators. Another possible source of false events is contamination

of the incident beam by low-energy protons which may be scattered and detected in accidental coincidence. Data to be presented later show that there was no significant low-energy component in the beam.

Another type of event is potentially very troublesome because it leads to a prompt coincidence of two low-energy protons, namely one in which both protons from a p - p elastic scattering penetrate slit edges and are scattered into their respective counter telescopes with degraded energy. In this way a $(45^\circ, 45^\circ)$ elastic scattering from the region just beyond the active volume could

TABLE I. Geometry for PPB measurements. Dimensions are in inches. The polar angles are those for the extreme rays in the plane of Fig. 2 which just graze the slit edges. The azimuthal angles are those subtended by the rear aperture as seen from the nearest point along the beam line.

Run	Front aperture		Rear aperture			Limits of angular acceptance	
	Width	Distance from center of chamber	Width	Height	Distance from center of chamber	Polar	Azimuthal
Large-aperture	0.178	2.69	0.30	1.65	7.81	$\pm 2.7^\circ$	$\pm 12.1^\circ$
Small-aperture	0.178	2.69	0.30	0.40	7.81	$\pm 2.7^\circ$	$\pm 2.9^\circ$

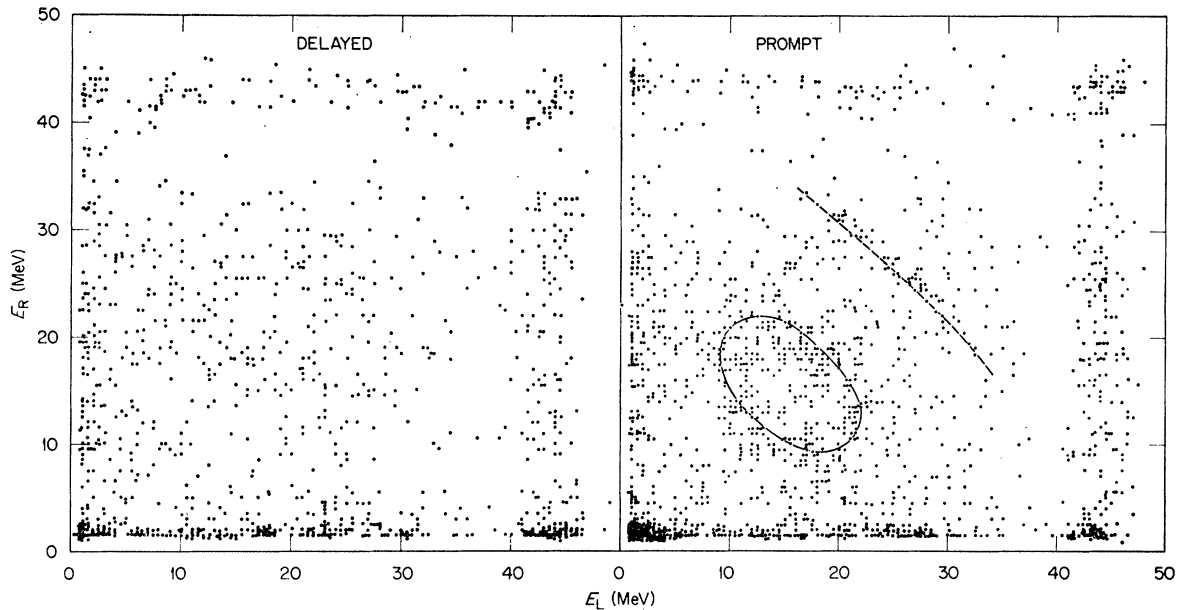


FIG. 3. Energy distribution of coincident events for the large-aperture geometry. The labels E_L and E_R refer to the energy deposited in the left and right stopping counters. The full curve is the kinematic locus of coplanar PPB events for $\theta_L = \theta_R = 30^\circ$, corrected for energy loss in the ΔE counters. The dashed curve is the corrected locus of coplanar proton pairs from the reaction $D(p, 2p)n$.

lead to a prompt coincidence of two low-energy protons. Evidence for detection of such events was found when the telescopes were both placed at 35° and at 40° . A pair of baffles (B in Figs. 1 and 2) was installed to stop such protons.

The number of 30° elastic protons entering each telescope was recorded by separate $(\Delta E, E)$ coincidence circuits with thresholds low enough to register all elastic protons. These numbers were useful both as a check on the apparatus (they should be equal) and for calculating the PPB cross section from the known p - p elastic cross section.

III. RESULTS AND DISCUSSION

The raw data for the large aperture run are shown in Fig. 3, with the prompt events on the right. The kinematic locus predicted for $(30^\circ, 30^\circ)$ coplanar PPB events, after correction for energy loss in the ΔE counters, is shown by the closed curve. The dashed curve shows the expected location of pairs of protons from breakup of the deuteron impurity in the target gas. The energy scale was derived from the elastic pulse height on the assumption that the system response was

linear. A subsequent study with the same counters substantiated this assumption.

Grouping of prompt events around the expected PPB and $D(p, 2p)n$ loci is evident, as is the lack of such grouping in the delayed-coincidence distribution. The events near 45 MeV involve coincidences between unrejected elastic protons. The absence of any clustering of delayed coincidences along the line $E_L = E_R$ (aside from the group near $E_L = E_R = 45$) indicates that the beam did not contain any significant low-energy components. A much more sensitive test was made by setting the counters to accept elastic coincidences. Again, no evidence was found for low-energy protons in the beam.

Figure 4 shows the distribution of events after subtraction of random coincidences. This was accomplished by cancelling each delayed event against the prompt coincidence nearest to it, provided they were within 5 MeV. The uncanceled delayed events are shown by crosses. The PPB and deuteron-breakup events stand out clearly. The number of events in the PPB region is given in the first line of Table II. The extent of the PPB region was determined by the en-

TABLE II. Data for $(30^\circ, 30^\circ)$ PPB measurements at 61.7 MeV. The column labeled "corrected" gives the experimental results after correction for acceptance of noncoplanar events on the assumption that they are distributed according to (4).

Run	Beam current (nA)	Length of run (h)	Counts in PPB region			Cross section in $\mu\text{b}/\text{sr}^2$		
			Prompt	Delayed	Net	Uncorrected	Corrected	Theoretical ^a
Large-aperture	40,80	45	330	82	248 ± 34	1.27 ± 0.20	2.38 ± 0.38	2.4
Small-aperture	200	13	44	19	25 ± 13	2.2 ± 1.2	2.3 ± 1.3	2.4

^a Coplanar result from Ref. 18.

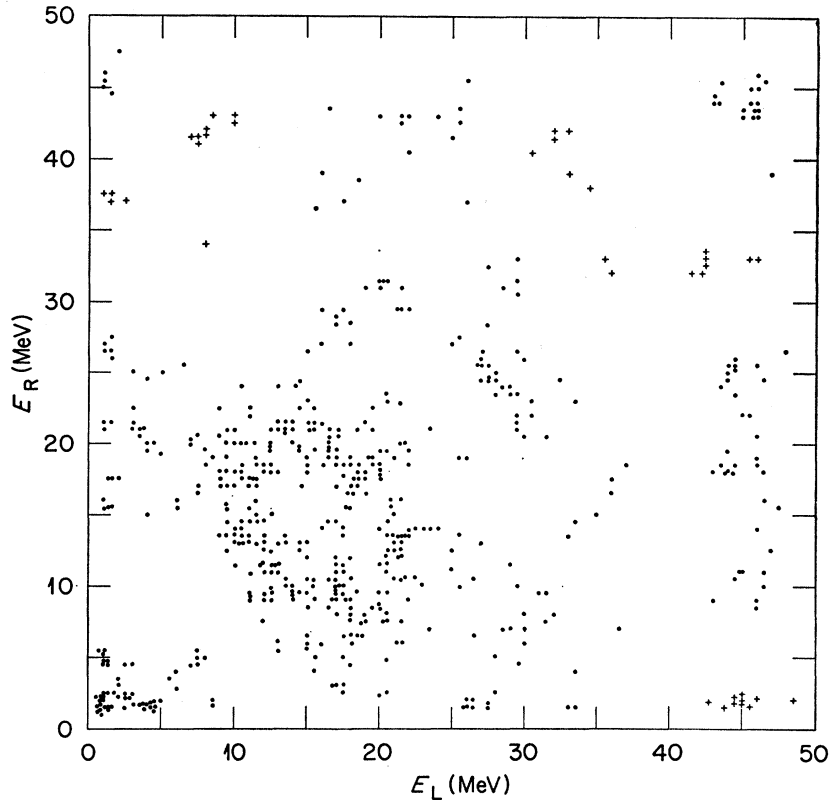


FIG. 4. Energy distribution of net events from Fig. 3. Uncanceled delayed events are shown by crosses.

velope of coplanar kinematic rings for all pairs of (θ_L, θ_R) angles at which PPB events could be accepted. The quoted error includes the uncertainty due purely to counting statistics combined with an estimate of the uncertainty in determining which counts to include, the latter arising mainly from the finite energy resolution. The apparent clusters of crosses or dots along the 45-MeV lines are probably statistical artifacts of the subtraction method since cancellations were always made between nearest neighbors.

As a check of the apparatus, the chamber was filled with $\frac{1}{2}$ atm each of methane and hydrogen, and the reaction $^{12}\text{C}(p, 2p)^{11}\text{B}$ was studied at cyclotron energies of 61.8 and 51.1 MeV. For final-state protons differing in energy by 5 MeV or less, the cross sections were found to be 14.7 and 13.1 $\mu\text{b}/\text{sr}^2 \text{MeV}$, respectively. The counting statistics were poor and no attempt was made to separate the ground state of ^{11}B from the 2.1-MeV excited state. Measurements by Pugh *et al.*¹³ at 50.0 MeV show that the 30° cross sections for the ground and 2.1-MeV states add up to about 11 $\mu\text{b}/\text{sr}^2 \text{MeV}$. The 51.1-MeV result agrees with this within its estimated accuracy ($\pm 20\%$).

The PPB cross section was calculated from the yield Y_{PPB} in two ways, (a) from the integrated beam and known geometry and (b) from the ratio of PPB events

to elastic protons. For the first method, the following expression was used:

$$\frac{d^2\sigma}{d\Omega_L d\Omega_R} = \frac{Y_{\text{PPB}}}{nNG_R\Delta\Omega_L/\sin\theta_R}, \quad (2)$$

where n =target atoms per unit volume, N =number of incident protons, G_R =geometry factor for right telescope, $\Delta\Omega_L$ =solid angle defined by left rear aperture, and θ_R =angle of right-telescope axis relative to beam direction. If A =area of rear aperture and R_0 =distance of rear aperture from target region, then $\Delta\Omega = A/R_0^2$. The geometry factor G is very nearly equal to wA/R_0h , where w =width of front slit and h =distance between front and rear slits. Silverstein's corrections¹⁴ to G for the finite size of the rear aperture and beam diameter were taken into account; they amounted to only about 0.6%. Corrections to G arising from the variation of cross section with angle¹⁴ were neglected. The effect of local beam heating on the target density n was estimated and found to be completely negligible. The combined uncertainty in quantities other than Y_{PPB} was estimated to be $\pm 7\%$.

To obtain Y_{PPB} it was necessary to correct the number of counts in Table II for the loss due to multiple Coulomb scattering in the ΔE detectors. This was calculated for various pairs of (E_L, E_R) energies on the

¹³ H. G. Pugh, D. L. Hendrie, M. Chabre, E. Boschitz, and I. E. McCarthy, Phys. Rev. **155**, 1054 (1967).

¹⁴ E. A. Silverstein, Nucl. Instr. Methods **4**, 53 (1959).

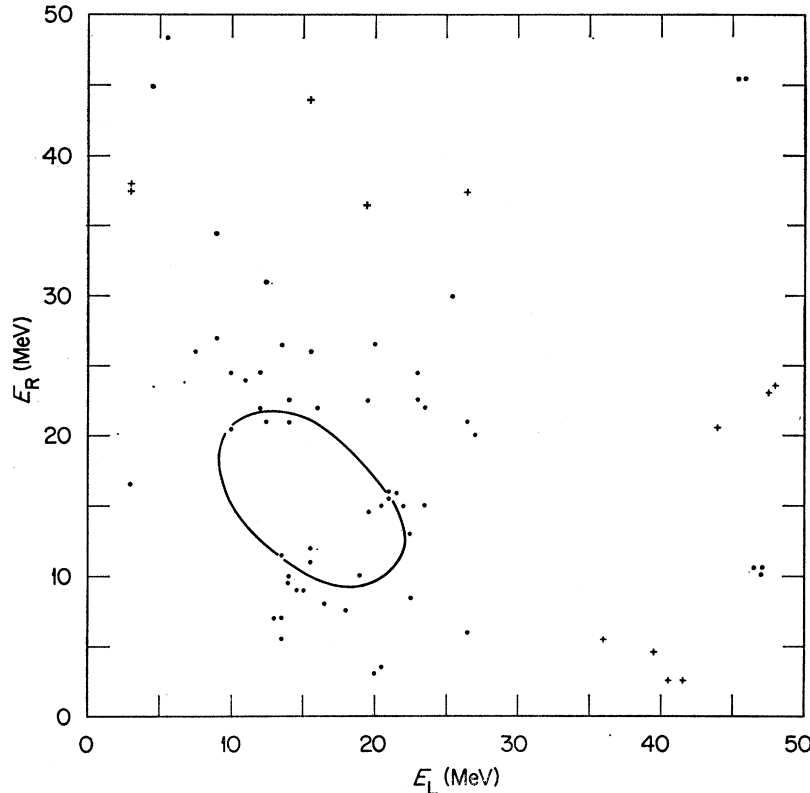


FIG. 5. Energy distribution of net coincident events for the small-aperture geometry. Points below 2 MeV are not shown. Uncancelled delayed events are shown by crosses. The curve is the kinematic locus of coplanar PPB events for $\theta_L = \theta_R = 30^\circ$.

kinematic locus. Even though the rms scattering angle is comparable with the half-width of the rear slits, the net scattering loss was small because of compensation by inscattering. The correction factor varied from 1.02 for the highest energies to 1.04 for the lowest; the number of counts was multiplied by 1.03 to obtain Y_{PPB} . The cross section calculated according to (2) is $1.22 \pm 0.20 \mu\text{b}/\text{sr}^2$. The error is dominated by the uncertainty in the number of counts.

A determination of the cross section independent of the errors in G , n , and N was obtained from the ratio of PPB counts to 30° elastic-proton yield and the known p - p elastic cross section by means of the relation

$$\frac{d^2\sigma}{d\Omega_L d\Omega_R} = \left(\frac{d\sigma}{d\Omega} \right)_{el} \frac{Y_{\text{PPB}}}{(Y_{el})_R} \frac{F}{\Delta\Omega_L}, \quad (3)$$

where $F=1.24$ is a geometrical correction necessary because the effect of the shadowing of the rear aperture by the front slit is different for singles and coincidences. In the penumbra, the detection efficiency for singles goes down linearly with position along the beam axis, while for coincidences it falls off quadratically. The small portions of the target volume visible to only one telescope (see Fig. 2) have a negligible effect on F in this geometry. The p - p elastic cross section was estimated to be $24 \text{ mb}/\text{sr}$ (lab) by interpolation between the 30°

results at 49.41^{15} and 68.30 MeV^{16} . The combined uncertainty in quantities other than Y_{PPB} was again estimated to be about $\pm 7\%$. From (3), the PPB cross section is $1.33 \pm 0.21 \mu\text{b}/\text{sr}^2$, in satisfactory agreement with the result from (2). The value quoted in the first line of Table II is the average of these two results.

Most predictions from theory have been for coplanar events only. Interpretation of the experimental results in terms of an equivalent coplanar cross section is difficult because the maximum possible noncoplanarity of the protons, $\Phi_m = 11.86^\circ$, is comparable with the $\pm 12.1^\circ$ vertical acceptance of the detector apertures. That is, if one proton goes through the center of one E counter, it is kinematically possible for the other proton to go above or below the center of the other E counter by as much as 11.86° and still be detected. The measurements thus involve a summation over the azimuthal angles φ_L and φ_R , and some knowledge or hypothesis about the φ dependence of the cross section is needed. Warner⁶ evaluated a correction for this effect by assuming that the matrix elements are independent of φ . With this assumption, the cross section in the first line of Table II should be multiplied by 1.295 to obtain the equivalent coplanar result,¹⁷ which gives an integrated

¹⁵ C. J. Batty, T. C. Griffith, D. C. Imrie, G. J. Lush, and L. A. Robbins, Nucl. Phys. A98, 489 (1967).

¹⁶ D. E. Young and L. H. Johnston, Phys. Rev. 119, 313 (1960).

¹⁷ W. T. H. van Oers (private communication).

coplanar cross section of $1.65 \pm 0.26 \mu\text{b}/\text{sr}^2$. This is somewhat lower than the 48-MeV result⁶ of 2.12 ± 0.36 and the 46-MeV result⁷ of 3.3 ± 1.4 , which were corrected in the same way.

The distribution of PPB events in Fig. 4 suggests, however, that the cross section is peaked toward coplanar events since the density of points is very low near the center of the PPB region. Measurements at 158 MeV show that the cross section decreases smoothly to zero at the kinematic limit of noncoplanarity.⁴ A similar effect is suggested by the data at 204 MeV.¹⁰ Pearce, Gale, and Duck¹⁸ have made a theoretical prediction of this distribution which agrees with the experimental data. A similar result has been obtained by Drechsel and Maximon.¹⁹ The predicted curve seems to be well represented by the parabola

$$\begin{aligned} f(\Phi) &= 1 - (\Phi/\Phi_m)^2, & |\Phi| < \Phi_m \\ &= 0, & |\Phi| \geq \Phi_m \end{aligned} \quad (4)$$

where Φ_m is the maximum value of Φ allowed by the kinematics.²⁰ If the Φ distribution at 61.7 MeV is assumed to be given by (4), then the measured large-aperture cross section would have to be multiplied by 1.88 to obtain the coplanar result. The correct cross section is shown in the first line of Table II. However, if $f(\Phi)$ is assumed to decrease linearly to zero, the correction factor would be 2.44; this triangular distribution is also consistent with the data of Ref. 4.

To decrease the uncertainty in this noncoplanarity correction, the vertical apertures of the rear counters were reduced to less than one-fourth of their former height, as indicated in the second line of Table I. The data are shown in Fig. 5 together with the coplanar kinematic ring. Time was available for only a short run so that only 25 net counts were accumulated in the PPB region. The cross sections calculated from (2) and (3) were again in good agreement, and their average is given in the second line of Table II, together with the equivalent coplanar cross section. The latter has been corrected by the factor 1.04, which was obtained by assuming that $f(\Phi)$ is given by (4). The factor would be 1.20 for the triangular distribution.

The corrected cross sections of Table II for both the large- and small-aperture data are in good agreement with the theoretical prediction of Pearce, Gale, and Duck¹⁸ given in Table II. They are also in reasonable agreement with recent results of several authors.^{19,21-23} On the other hand, the predictions of Ref. 24, if inter-

¹⁸ W. A. Pearce, W. A. Gale, and I. Duck, Nucl. Phys. **B3**, 241 (1967).

¹⁹ D. Drechsel and L. C. Maximon (to be published).

²⁰ The angle of noncoplanarity used in Ref. 18 is $\varphi_L - \varphi_R$ rather than $\varphi_L - \varphi_R - 180^\circ$.

²¹ V. R. Brown, Phys. Letters **25B**, 506 (1967); and (private communication).

²² A. H. Cromer (to be published).

²³ P. S. Signell, in *Symposium on Light Nuclei, Few-Body Problems, and Nuclear Forces, Yugoslavia, 1967* (Gordon and Breach Science Publishers, Inc., New York, to be published in 1968).

²⁴ M. I. Sobel and A. H. Cromer, Phys. Rev. **158**, 1157 (1967).

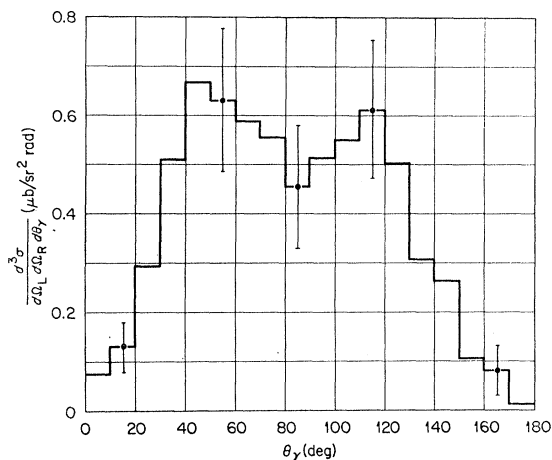


FIG. 6. Distribution of PPB events as a function of γ -ray angle for the large-aperture geometry. These data were obtained from Fig. 4, as described in the text. Typical standard deviations are shown for the number of counts in each bin. The cross sections near 0° and 180° are probably too small for the reasons given in the text.

polated to 61.7 MeV, would give a cross section about four times larger than the experimental result. This discrepancy is now understood.^{19,22,23} The calculations of Ref. 24 were done in the laboratory system and the double-scattering term was ignored. In such calculations a portion of the single-scattering contribution is very large below 100 MeV, but this is cancelled by part of the double-scattering term. If double scattering is included in the laboratory-system calculations, the cross section is in much better agreement with experiment.²² For calculations in the center-of-mass system,^{18,19,21,23} this problem does not arise.

The distribution of PPB events as a function of the γ -ray polar angle θ_γ is shown by the histogram in Fig. 6. To obtain this result, a detailed treatment of the kinematics was necessary. For noncoplanar events θ_γ cannot be 0° or 180° , and its range steadily shrinks to a single point as Φ increases to the kinematic limit. Figure 7 shows loci of constant θ_γ (dashed lines) and constant Φ (full and dotted lines) for $\theta_L = \theta_R = 30^\circ$. Similar curves were constructed at 10° intervals in θ_γ for all possible pairs of (θ_L, θ_R) angles, not necessarily equal, in increments of 1° . The constant- θ_γ loci were corrected for energy loss in the ΔE detectors and superposed on a plot similar to Fig. 4. The number of net data points in each θ_γ band was counted for each superposition. The resulting θ_γ distributions were combined with weighting proportional to the relative geometrical efficiency for each (θ_L, θ_R) pair. The combined distribution was then normalized and plotted in Fig. 6 as $d^3\sigma/d\Omega_L d\Omega_R d\theta_\gamma$. The normalization corresponds to an area of $1.19 \mu\text{b}/\text{sr}^2$, one-half of the corrected value of $d^2\sigma/d\Omega_L d\Omega_R$ in Table II, since the 0° to 180° range of θ_γ is covered twice because of the symmetric geometry.

In the unfolding procedure described above, it was assumed that $d^3\sigma/d\Omega_L d\Omega_R d\theta_\gamma$ is independent of θ_L and

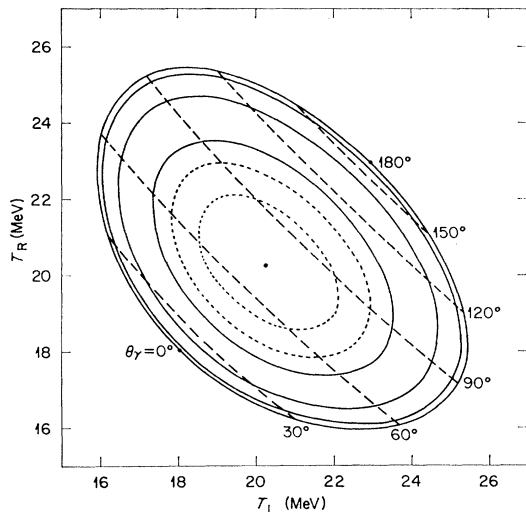


FIG. 7. Kinematics for noncoplanar PPB events with a 61.7-MeV beam for proton polar angles of 30.0° . The full curves show the allowed proton kinetic energies T_L and T_R for constant Φ . The outermost ring is for $\Phi=0$ (coplanar events). The others, in order of decreasing size, are for $\Phi=3^\circ$, 6° , and 9° . The dotted curves are for $\Phi=10^\circ$ and 11° , while the dot near the center is for the event of maximum possible noncoplanarity, $\Phi=11.86^\circ$. The dashed lines are loci of constant θ_γ .

θ_R for the pairs of angles which contribute. With this assumption, the procedure is unambiguous provided that the energy resolution is perfect and there is no multiple scattering. For the present data, the spread of the E_L and E_R pulse heights corresponds to one-third to one-half of the spread in energies due to the finite angular acceptance. Thus the distortion of $d^3\sigma/d\Omega_L-$

$d\Omega_R d\theta_\gamma$ introduced by the finite energy resolution should include a weakening of the maxima and filling in of the central minimum. In addition, some of the counts which ought to be in the 0° and 180° regions may appear elsewhere because the bands in Fig. 7 corresponding to these regions have very small area. The effects of multiple scattering should be similar.

The histogram in Fig. 6 is in general agreement with recent theoretical predictions for coplanar events.^{19,21-23} The experimental cross section near 0° and 180° is smaller than the predictions, partly because of the effects mentioned just above, and partly because of acceptance of noncoplanar events, none of which give contributions for $\theta_\gamma=0^\circ$ or 180° .

[*Note added in proof.* Drechsel and Maximon²⁵ have calculated the variation of $d^2\sigma/d\Omega_L d\Omega_R$ with Φ at 62 MeV for the Hamada-Johnston potential. The correction factors for noncoplanarity obtained from their distribution are 1.609 for the large-aperture geometry and 1.020 for the small-aperture geometry. The corresponding coplanar cross sections are 2.04 and 2.24 $\mu\text{b}/\text{sr}^2$, respectively.]

ACKNOWLEDGMENTS

We wish to thank B. Gottschalk and A. Zucker for bringing this problem to our attention, R. E. Warner for helpful suggestions at the outset of our work, A. H. Cromer for many useful discussions, and D. O. Galde and A. R. Quinton for assistance in data taking. We also wish to thank the ORIC operations staff for their excellent cooperation.

²⁵ D. Drechsel and L. C. Maximon (private communication).